Kinetic isotope effects and transition state structure for human phenylethanolamine *N*-methyltransferase

Christopher F. Stratton, Myles B. Poulin, Quan Du, & Vern L. Schramm*

Department of Biochemistry, Albert Einstein College of Medicine,
1300 Morris Park Avenue, Bronx, New York 10461, United States

Supporting Information

A. SUPPORTING INFORMATION FIGURES S1–S5

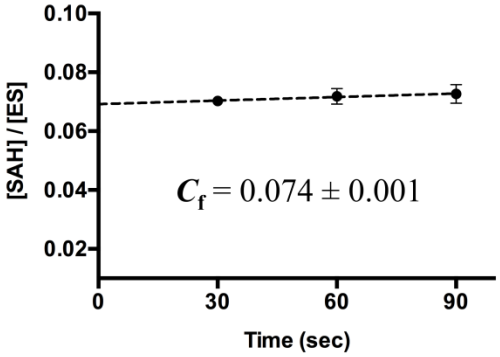

Figure S1. Forward commitment (C_f) for the hPNMT reaction. C_f was measured by the substrate trapping method[1] using [8-^{14}C]SAM. hPNMT, human phenylethanolamine *N*-methyltransferase; SAH, *S*-adenosyl-L-homocysteine; ES, hPNMT▪*S*-adenosyl-L-methionine complex; SAM, *S*-adenosyl-L-methionine.

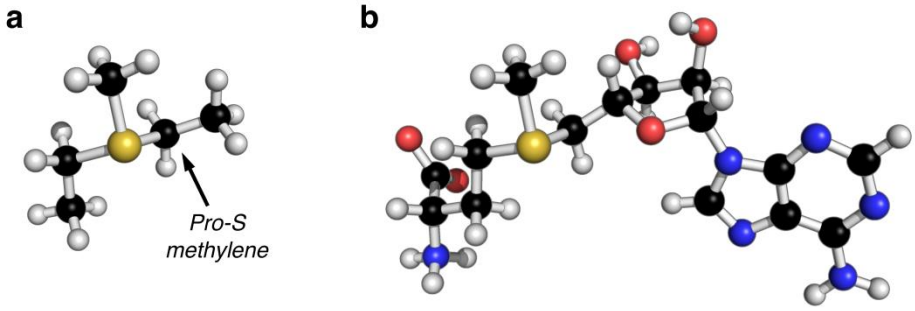

Figure S2. GS model for SAM used in the KIE calculations. (a) Minimized structure (Gaussian 09, RB3LYP/6-31g(d) theory)[2] of the diethyl(methyl)sulfonium GS used in the TS analysis. Values for the 5′-$^{3}H_2$ and 5′-^{14}C KIEs were calculated for the *pro-S* methylene group of the diethyl(methyl)sulfonium model, as this position corresponds to the 5′ carbon in the full SAM structure. (b) Full structure of the low-energy conformer of SAM taken from the PubChem database.[3] GS, ground state; SAM, *S*-adenosyl-L-methionine; KIE, kinetic isotope effect; TS, transition state. Atom colors are: hydrogen, white; carbon, black; oxygen, red; nitrogen, blue; sulfur, yellow.

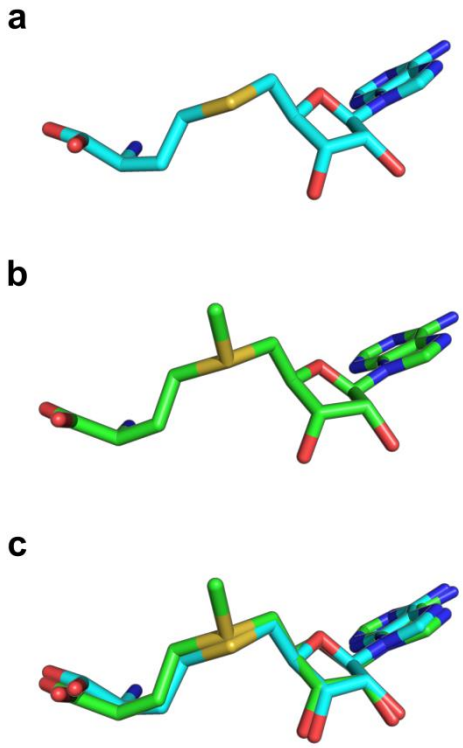

Figure S3. Conformation of SAH and SAM when bound to hPNMT. (a) Structure of SAH in ternary complex with hPNMT and norepinephrine; coordinates taken from PDB: 3HCD.[4] (b) Structure of SAM in ternary complex with hPNMT and the inhibitor 3-hydroxymethyl-7-nitro-THIQ; coordinates taken from PDB: 2G70.[5] (c) Overlay of bound structures for SAH (PDB: 3HCD)[4] and SAM (PDB: 2G70).[5] SAH, *S*-adenosyl-L-homocysteine; SAM, *S*-adenosyl-L-methionine; hPNMT, human phenylethanolamine *N*-methyltransferase; PDB, protein databank.

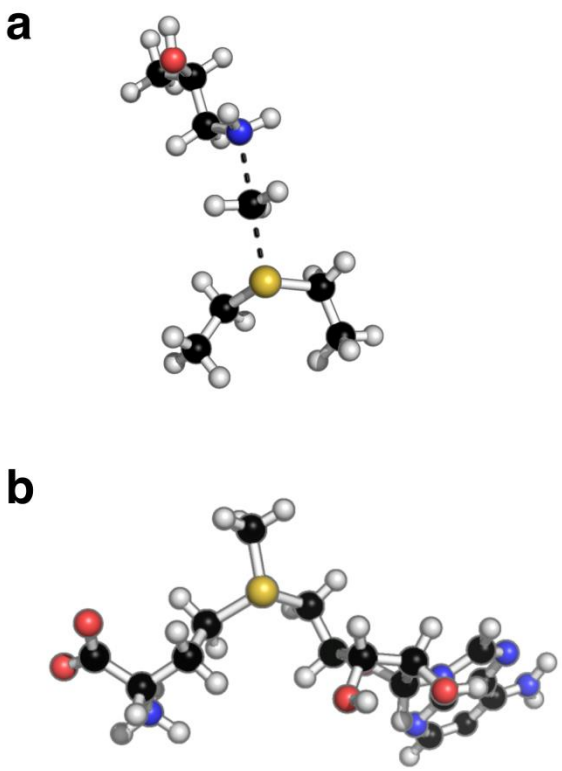

Figure S4. Comparison of TS structure model and bound conformation of SAM. (a) TS structure model for hPNMT shown in Figure 2 of the main text. (b) Structure of SAM in ternary complex with hPNMT and the inhibitor 3-hydroxymethyl-7-nitro-THIQ; coordinates taken from PDB: 2G70.[5] TS, transition state; SAM, *S*-adenosyl-L-methionine; hPNMT, human phenyl-ethanolamine *N*-methyltransferase; PDB, protein databank. Atom colors are: hydrogen, white; carbon, black; oxygen, red; nitrogen, blue; sulfur, yellow.

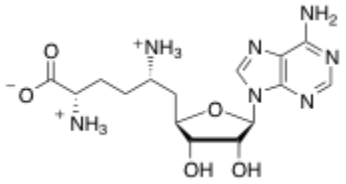

Figure S5. Structure of the methyltransferase inhibitor sinefungin.

B. SUPPORTING INFORMATION TABLE S1 AND TABLE S2

	Bond length in TS model (Å)			Bond order in TS model		
	hPNMT	NSD2[b]	DNMT1[c]	hPNMT	NSD2[b]	DNMT1[c]
C_{Me}–S	2.26	2.53	2.29	0.62	0.38	0.52
C_{Me}–N(C^a)	2.18	2.10	2.22	0.31	0.48	0.34

Table S1. Bond lengths and bond orders for the hPNMT TS structure model. Values for hPNMT correspond to the TS structure shown in Figure 2 of the main text. [a]In the case of DNMT1, the methyl-acceptor is C5 of cytosine. [b]Values taken from Poulin *et al*.[6] [c]Values taken from Du *et al*.[7] TS, transition state; hPNMT, human phenylethanolamine *N*-methyltransferase.

	GS	TS	Δ (TS–GS)
S	0.896	0.547	–0.349
CH_3	0.017	0.205	0.188

Table S2. NBO calculations for the GS structure of the diethyl(methyl)sulfonium SAM mimic and the hPNMT TS model. Charge values for the sulfur (S) of SAM and the transferring methyl group (CH_3) were read directly from the .log file of the NBO calculations. Charges values for CH_3 are the sum of the individual charges on the methyl carbon atom and each proton. GS, ground state; TS, transition state; NBO, natural bond orbital; SAM, *S*-adenosyl-L-methionine.

C. METHODS

Expression and purification of wild-type hPNMT. A synthetic gene was designed for hPNMT (NCBI Gene ID: 5409) and purchased from DNA2.0 Inc. (Menlo Park, CA) in a pJexpress414 expression vector. The *N*-terminus of the encoded protein was modified with the addition of 19 amino acids, including a His_6 tag and a thrombin cleavage site. Conditions for the heterologous expression of hPNMT in *E. coli* (One Shot® BL21 Star™ (DE3) cell line) and purification were adapted from Qian *et al.*[8] Briefly, a 25 mL starter culture in LB-ampicillin (100 μg/mL) medium was incubated overnight at 37 °C. The next day, 12 mL of the starter culture was diluted in 2 L of fresh LB-ampicillin (100 μg/mL) and incubated at 37 °C to OD_{600} = 0.6. Protein expression was induced by the addition of 1 mM isopropyl-D-thiogalactoside and the culture was incubated overnight at 28 °C. The next day, cells were harvested via centrifugation and resuspended in 30 mL of Buffer A (50 mM sodium phosphate, 300 mM NaCl, 10 mM imidazole, pH = 8.0). Lysozyme and DNAse were added to the cell suspension and the mixture was incubated at 4 °C for 40 min. Cells were lysed via sonication and cell debris was removed by centrifugation. Cleared cell lysate was poured over a column of Ni-NTA resin (Qiagen), which had been pre-equilibrated with Buffer A. The resin was washed with five column volumes of Buffer A and the protein was eluted with a step gradient of imidazole (30 mM, 50 mM, 100 mM, 250 mM, and 500 mM) in the same buffer system. Fractions containing hPNMT were identified via SDS-PAGE, pooled, and exchanged into 20 mM Tris–HCl, 1 mM EDTA, 0.5 mM DTT, 15% glycerol v/v, pH = 7.2 via dialysis. The pure protein was concentrated to 149 μM and stored at –80 °C.

Synthesis of isotopically labeled SAM substrates. Seven SAM substrates were prepared as previously described[6,7] with isotopes incorporated at either isotopically sensitive ([*methyl*-$^3H_3$], [*methyl*-^{14}C], [^{36}S, 8-^{14}C], [5′-$^3H_2$], and [5′-^{14}C]) or remote positions ([1′-^3H] and [8-^{14}C]). The SAM substrates were accessed via a chemoenzymatic approach in which ATP intermediates were synthesized in 4–7 enzymatic steps from isotopically labeled commercial material. The ATP intermediates were purified and used to synthesize the corresponding SAM substrates using the human SAM synthetase MAT2A, as summarized in the schematic below.

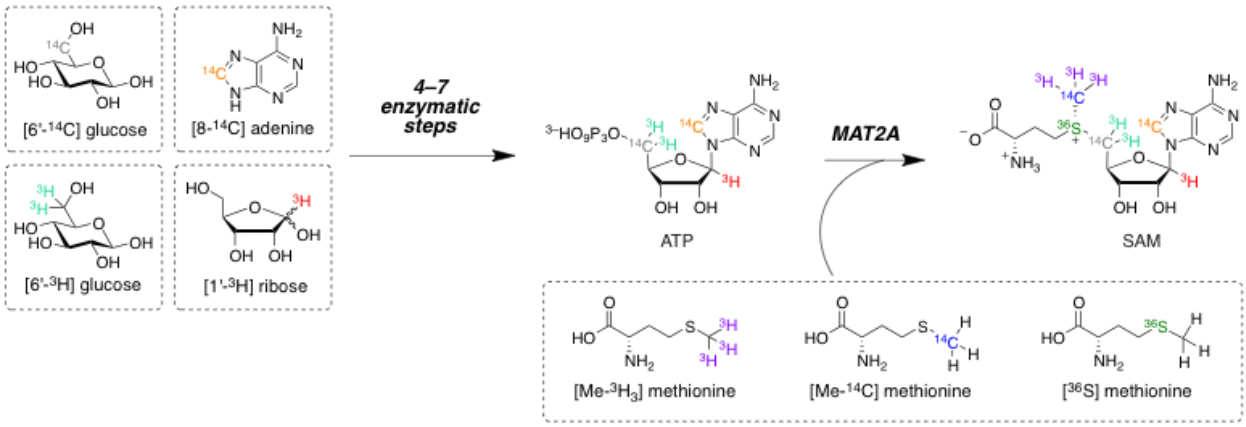

Schematic overview of synthetic route to isotopically labeled SAM substrates. The colored positions indicate where individual isotopes were incorporated into separate SAM molecules. ATP, adenosine triphosphate; SAM, *S*-adenosyl-L-methionine; MAT2A, human SAM synthetase.

Synthesis of isotopically labeled ATP intermediates. Synthesis of the ATP intermediates was carried out as previously described.[9] [5′-$^{3}H_2$]ATP and [5′-^{14}C]ATP were prepared from [6′-^{3}H]glucose and [6′-^{14}C]glucose, respectively. The conditions for these syntheses were: 2 mM glucose (total concentration of labeled + unlabeled glucose), 2.1 mM adenine, 100 µM ATP, 10 mM $MgCl_2$, 5 mM $NADP^+$, 30 mM phosphoenolpyruvate (PEP), 50 mM KCl, 100 mM phosphate buffer (pH 7.4), with 1 U·mL^{-1} hexokinase (HK), 5 U·mL^{-1} myokinase (MK), 1 U·mL^{-1} glucose-6-phosphate dehydrogenase (G6PD), 1 U·mL^{-1} 6-phosphogluconate dehydrogenase (6PGD), 5 U·mL^{-1} phosphoriboisomerase (PRI), 10 U·mL^{-1} pyruvate kinase (PK), 5 U·mL^{-1} phosphoribosylpyrophosphate synthetase (PRPPase), and 5 U·mL^{-1} adenine phosphoribosyltransferase (APRTase).

[1′-^{3}H]ATP was prepared from [1′-^{3}H]ribose using the conditions: 2.0 mM ribose (total concentration of labeled + unlabeled ribose), 2.1 mM adenine, 0.1 mM ATP, 30 mM PEP, 10 mM $MgCl_2$, 50 mM KCl, 100 mM phosphate buffer (pH 7.4), with 5 U·mL^{-1} RK, 2 U·mL^{-1} MK, 10 U·mL^{-1} PK, 5 U·mL^{-1} PRPPase, and 2 U·mL^{-1} APRTase.

[8-^{14}C]ATP was prepared from [8-^{14}C]adenine using the conditions: 2 mM adenine (total concentration of labeled + unlabeled adenine), 2.5 mM PRPP, 50 µM ATP, 30 mM PEP, 10 mM $MgCl_2$, 50 mM KCl, 100 mM phosphate buffer (pH 7.4), with 2 U·mL^{-1} MK, 20 U·mL^{-1} PK, and 2 U·mL^{-1} APRTase.

Synthesis of isotopically labeled SAM substrates. Labeled SAM substrates were enzymatically synthesized as previously described[6,7] from the corresponding ATP intermediates or labeled methionines using the human methionine adenosyltransferase MAT2A. The MAT2A protein was heterologously expressed in *E. coli* and purified in a manner consistent with previous reports.[10] [^{36}S]methionine was prepared from [^{36}S]sulfur via a chemoenzymatic synthesis as previously reported by Poulin *et al.*[11] A typical reaction was incubated at 37 ºC for 3 hr and contained 4 μM MAT2A, 1 mM ATP, and 1 mM methionine in 50 mM Tris–HCl, 50 mM KCl, and 10 mM $MgCl_2$ (pH 8.0). Labeled SAM substrates were purified via reverse phase HPLC using a H_2O–acetonitrile gradient with 0.1% formic acid.[6,7]

Measurement of *V/K* KIEs for the hPNMT reaction. KIEs on the hPNMT reaction were measured at 30 °C using the competitive radiolabel approach.[12,13] Reaction conditions for the KIE measurements were: 50 mM potassium phosphate, 50 μM norepinephrine, 50 μM SAM ([*heavy label*]SAM + [*remote label*]*p*ABA + unlabeled carrier), 1 μM hPNMT, pH = 8.0. For a typical KIE measurement, a master mix containing all reaction components (except hPNMT) was prepared and distributed into equivolume aliquots. Then, hPNMT was added to aliquots designated as 'experimental reactions' and an equivalent volume of buffer was added to aliquots designated as 'no-enzyme controls.' The hPNMT reaction was allowed to proceed to ~40–60% completion and then quenched by the addition of H_2SO_4 to a final concentration of 10 mM. SAM and SAH were purified from the quenched reaction mixtures via reverse phase HPLC (Phenomenex Gemini, 5 μm C-18 110 Å, 4.6 x 250 mm). The buffers used in this purification were 50 mM ammonium acetate at pH = 4.3 (Buffer B) and 0.1% acetic acid in 50% acetonitrile (Buffer C). The method used was 100% Buffer B at 1 mL/min for 6 min followed by a linear gradient of 0–100% Buffer C over 14 min (Method 1). Under these conditions, the peaks corresponding to SAM and SAH eluted at approximately 6 min and 17 min, respectively. Purified SAM and SAH samples from the KIE reactions were evaporated to dryness by centrifugation under vacuum in 20 mL scintillation vials. To each vial was then added 500 μL of H_2O and 10 mL of Ultima Gold™ scintillation fluid (PerkinElmer).

Scintillation counting was performed on each sample over 10 cycles at 10 min/cycle using a Tri-carb 2910TR scintillation counter (PerkinElmer), which is a dual-channel instrument that registers the signal for ^{3}H in Channel A and the signal for ^{14}C in both Channel A and Channel B.

As such, the raw data must be deconvoluted to determine the total counts for ^{3}H-labeled SAM and ^{14}C-labeled SAM. A control sample of ^{14}C-labeled SAM was used to determine the proportion of signal overlap between Channel A and Channel B for ^{14}C, as defined by eq 2:

$$r = \text{Channel A} / \text{Channel B} \quad (2)$$

Spectral deconvolution of the KIE data was achieved for ^{3}H and ^{14}C using eq 3 and eq 4, respectively:

$$^{3}\text{H} = \text{Channel A} - (\text{Channel B} \times r) \quad (3)$$

$$^{14}\text{C} = \text{Channel B} + (\text{Channel B} \times r) \quad (4)$$

V/K KIE values were calculated from eq 5, where R_0 and R_f are the ratios of [*labeled*]SAM to [*unlabeled*]SAM prior to the reaction (*i.e.*, no-enzyme control) and at partial conversion (respectively), and f is the fraction of substrate conversion.

$$\text{KIE}_{V/K} = \ln(1 - f) / \ln[(1 - f) \times (R_f / R_0)] \quad (5)$$

Measurement of forward commitment for the hPNMT reaction. Forward commitment for SAM in the hPNMT reaction was measured using the isotope trapping method.[1] A 20 uL sample of the hPNMT▪SAM equilibrium complex (ES) was formed by incubating 10 μM hPNMT with 20 μM [8-^{14}C]SAM for 15 min in 50 mM potassium phosphate (pH = 8.0) at 30 ºC. A chase solution (480 μL; 2.67 mM unlabeled SAM, 52 μM norepinephrine, 50 mM potassium phosphate, pH = 8.0) was pre-heated to 30 ºC and rapidly mixed with the ES complex solution. Three 150 uL aliquots were removed from the mixture and quenched with 10 mM H_2SO_4 (final concentration) at 30, 60, and 90 seconds. Control reactions containing no norepinephrine in the chase solution were processed in parallel to correct for background levels of SAM breakdown at 30 ºC. SAM and SAH were purified from the quenched reactions via HPLC Method 1. Purified samples were evaporated to dryness in 20 mL scintillation vials via centrifugation under vacuum. Dried samples were then dissolved in 500 uL of H_2O and 10 mL of Ultima Gold^{TM} scintillation

fluid (PerkinElmer). Scintillation counting and spectral deconvolution were performed as described for the KIE measurements. The ratio of SAH produced to the initial concentration of ES complex was plotted as a function of time and extrapolated to time = 0 (Figure S1). C_f was calculated using eq 6, where Y is the ratio of SAH produced to the initial concentration of ES complex at time = 0. The concentration of the ES complex was calculated using eq 7, where E is the concentration of hPNMT, S is the concentration of SAM, and K_M is the Michaelis constant for SAM (taken from Wu *et al*[14]).

$$C_f = Y / (1 - Y) \quad (6)$$

$$ES = (E \times S) / (S + K_M) \quad (7)$$

Computational methods. The hPNMT TS structure was modeled via DFT calculations using the B3LYP functional and 6-31g(d) basis set as implemented in Gaussian 09.[2] KIEs were calculated at 30 ºC (TKELV = 303.15) using ISOEFF98[15] from the scaled vibrational frequencies (SCFACT = 0.977) of optimized structures for SAM in the GS and each TS structure, as detailed below.

The input coordinates for the optimization of SAM in the GS were taken from the PubChem 3D database (CID: 24762165).[3] The fully elaborated SAM structure was truncated to the diethyl(methyl)sulfonium species shown in Figure S2a, and an optimization was carried out using water as an implicit solvent model (PCM). The GS of SAM was modeled free in solution because the influence of protein binding on measured KIEs has not been experimentally investigated for hPNMT. However, recent studies on the human protein lysine methyltransferase NSD2[16] and glycine *N*-methyltransferase[17] suggest ternary complex binding isotope effects are within experimental error of unity. As such, these effects are not predicted to contribute appreciably to the KIE values. The optimized GS structure was located as the global minimum and displayed no imaginary frequencies. Values for the 5′-$^3H_2$ and 5′-^{14}C KIEs were calculated for the *pro-S* methylene group of the diethyl(methyl)sulfonium model, as this position corresponds to the 5′ carbon in the full SAM structure (Figure S2).

All optimizations in the TS search used acetone as an implicit solvent model (PCM), and each TS structure displayed a single imaginary frequency corresponding to atomic motion along

the axis of methyl transfer. Initially, dihedrals for the ethyl groups of the diethyl(methyl) sulfonium model of SAM were fixed to their crystallographic values (PDB: 2G70).[5] TS structures were then calculated with the C_{Me}–N bond fixed at 2.0 Å and the C_{Me}–S bond fixed at 1.8, 2.0, 2.2, 2.4, 2.6, 2.8, 3.0, or 3.2 Å. The C_{Me}–S bond was then held fixed at each of these values, and TS structures were calculated with the C_{Me}–N bond fixed at 1.6, 1.8, 2.2, 2.4, 2.6, 2.8, 3.0, or 3.2 Å. TS structures were refined through optimizing structures with the C_{Me}–N bond length fixed at 2.15, 2.16, 2.17, 2.18, 2.19, or 2.20 Å and the C_{Me}–S bond length fixed at 2.23, 2.24, 2.25, 2.26, or 2.27 Å. After locating a candidate model, constraints on the dihedrals the diethyl(methyl)sulfonium SAM mimic were released and the structure was re-optimized at the same level of theory to arrive at the final structure shown in Figure 2 of the main text. Optimization of the final TS model fully converged and provided a single imaginary frequency of 476*i* cm^{-1} corresponding to atomic motion along the axis of methyl transfer.

```
         Item                 Value      Threshold   Converged?
Maximum  Force               0.000029     0.000450        YES
RMS      Force               0.000005     0.000300        YES
Maximum  Displacement        0.001337     0.001800        YES
RMS      Displacement        0.000398     0.001200        YES
Predicted change in Energy=-2.637144D-08
Optimization completed.
   -- Stationary point found.
```

NBO analysis and single point energy calculations were performed on optimized structures using the NBO3.0 program available in Gaussian 09. EPS maps in Figure 3 of the main text were visualized in GaussView 5.0 (isovalue = 0.04) from the electron density and potential cubes acquired from the checkpoint files of single point energy calculations. Bond orders were calculated based on Wiberg's formula.[2]

Input coordinates for sinefungin were taken from the lowest energy conformer in the PubChem 3D database (CID: 25246235).[3] The structure was optimized using water as an implicit solvent model and the electrostatic potential map shown in Figure 3 of the main text was generated as described above for the TS structure model.

D. SUPPORTING INFORMATION REFERENCES

(1) Rose, I. A. (1980) The isotope trapping method: desorption rates of productive E.S complexes. *Methods Enzymol. 64*, 47–59.

(2) Frisch, M. J. T., G. W.; Schlegel, H. B.; Scuseria, G. E.; Robb, M. A.; Cheeseman, J. R.; Scalmani, G.; Barone, V.; Mennucci, B.; Petersson, G. A.; Nakatsuji, H.; Caricato, M.; Li, X.; Hratchian, H. P.; Izmaylov, A. F.; Bloino, J.; Zheng, G.; Sonnenberg, J. L.; Hada, M.; Ehara, M.; Toyota, K.; Fukuda, R.; Hasegawa, J.; Ishida, M.; Nakajima, T. E.; Honda, Y.; Kitao, O.; Nakai, H.; Vreven, T.; Montgomery, J. A.; Peralta, J. E.; Ogliaro, F.; Bearpark, M.; Heyd, J. J.; Brothers, E.; Kudin, K. N.; Staroverov, V. N.; Kobayashi, R.; Normand, J.; Raghavachari, K.; Rendell, A.; Burant, J. C.; Iyengar, S. S.; Tomasi, J.; Cossi, M.; Rega, N.; Millam, J. M.; Klene, M.; Knox, J. E.; Cross, J. B.; Bakken, V.; Adamo, C.; Jaramillo, J.; Gomperts, R.; Stratmann, R. E.; Yazyev, O.; Austin, A. J.; Cammi, R.; Pomelli, C.; Ochterski, J. W.; Martin, R. L.; Morokuma, K.; Zakrzewski, V. G.; Voth, G. A.; Salvador, P.; Dannenberg, J. J.; Dapprich, S.; Daniels, A. D.; Farkas, O.; Foresman, J. B.; Ortiz, J. V.; Cioslowski, J.; Fox, D. J. (2009) Gaussian 09, Gaussian, Inc., Wallingford, CT.

(3) Kim, S.; Bolton, E. E.; Bryant, S. H. (2013) PubChem3D: conformer ensemble accuracy. *J. Cheminform. 5*, 1.

(4) Drinkwater, N.; Gee, C. L.; Puri, M.; Criscione, K. R.; McLeish, M. J.; Grunewald, G. L.; Martin, J. L. (2009) Molecular recognition of physiological substrate noradrenaline by the adrenaline-synthesizing enzyme PNMT and factors influencing its methyltransferase activity. *Biochem. J. 422*, 463–471.

(5) Gee, C. L.; Drinkwater, N.; Tyndall, J. D.; Grunewald, G. L.; Wu, Q.; McLeish, M. J.; Martin, J. L. (2007) Enzyme adaptation to inhibitor binding: a cryptic binding site in phenylethanolamine *N*-methyltransferase. *J. Med. Chem. 50*, 4845–4853.

(6) Poulin, M. B.; Schneck, J. L.; Matico, R. E.; McDevitt, P. J.; Huddleston, M. J.; Hou, W.; Johnson, N. W.; Thrall, S. H.; Meek, T. D.; Schramm, V. L. (2016) Transition state for the NSD2-catalyzed methylation of histone H3 lysine 36. *Proc. Natl. Acad. Sci. U.S.A. 113*, 1197–1201.

(7) Du, Q.; Wang, Z.; Schramm, V. L. (2016) Human DNMT1 transition state structure. *Proc. Natl. Acad. Sci. U.S.A. 113*, 2916–2921.

(8) Wu, Q.; Gee, C. L.; Lin, F.; Tyndall, J. D.; Martin, J. L.; Grunewald, G. L.; McLeish, M. J. (2005) Structural, mutagenic, and kinetic analysis of the binding of substrates and inhibitors of human phenylethanolamine *N*-methyltransferase. *J. Med. Chem. 48*, 7243–7252.

(9) Parkin, D. W.; Leung, H. B.; Schramm, V. L. (1984) Synthesis of nucleotides with specific radiolabels in ribose. Primary ^{14}C and secondary ^{3}H kinetic isotope effects on acid-

catalyzed glycosidic bond hydrolysis of AMP, dAMP, and inosine. *J. Biol. Chem. 259*, 9411–9477.

(10) Shafqat, N.; Muniz, J. R.; Pilka, E. S.; Papagrigoriou, E.; von Delft, F.; Oppermann, U.; Yue, W. W. (2013) Insight into *S*-adenosylmethionine biosynthesis from the crystal structures of the human methionine adenosyltransferase catalytic and regulatory subunits. *Biochem. J. 452*, 27–36.

(11) Poulin, M. B.; Du, Q.; Schramm, V. L. (2015) Chemoenzymatic synthesis of (36)S isotopologues of methionine and *S*-adenosyl-L-methionine. *J. Org. Chem. 80*, 5344–5347.

(12) Schramm, V. L. (1998) Enzymatic transition states and transition state analog design. *Annu. Rev. Biochem. 67*, 693–720.

(13) Schramm, V. L. (1999) Enzymatic transition-state analysis and transition-state analogs. *Methods Enzymol. 308*, 301–355.

(14) Wu, Q.; McLeish, M. J. (2013) Kinetic and pH studies on human phenylethanolamine *N*-methyltransferase. *Arch. Biochem. Biophys. 539*, 1–8.

(15) Anisimov, V. and Paneth, P. (1999) ISOEFF98. A program for studies of isotope effects using Hessian modifications. *J. Math Chem. 26*, 75–86.

(16) Poulin, M. B.; Schneck, J. L.; Matico, R. E.; Hou, W.; McDevitt, P. J.; Holbert, M.; Schramm, V. L. (2016) Nucleosome binding alters the substrate bonding environment of histone H3 lysine 36 methyltransferase NSD2. *J. Am. Chem. Soc. 138*, 6699–6702.

(17) Zhang, J., and Klinman, J. P. (2016) Convergent mechanistic features between the structurally diverse *N*- and *O*-methyltransferases: glycine *N*-methyltransferase and catechol *O*-methyltransferase, *J. Am. Chem. Soc. 138*, 9158–9165.